

The Integrity of Polymer Composites During and After Fire

A. G. GIBSON,* P. N. H. WRIGHT AND Y-S. WU
*Centre for Composite Materials Engineering, Stephenson Building
University of Newcastle upon Tyne, NE1 7RU, UK*

A. P. MOURITZ
*Department of Aerospace Engineering, RMIT University
The Sir Lawrence Wackett Centre for Aerospace Design Technology
GPO Box 2476V, Melbourne, Victoria, Australia 3001*

Z. MATHYS AND C. P. GARDINER
*Defence Science and Technology Organisation
Platforms Sciences Laboratory
P. O. Box 4331, Melbourne, Victoria, Australia 3001*

(Received September 23, 2003)
(Accepted December 17, 2003)

ABSTRACT: This paper reports on changes to the mechanical properties of woven glass laminates with polyester, vinyl ester and phenolic resins during fire exposure. Two sets of experiments were carried out. First, unstressed laminates were exposed to a constant one-sided heat flux (50 kW m^{-2}) for various times, and the residual post-fire strength at room temperature was reported.

In a second series of experiments, laminates were tested under load. The times corresponding to a given loss of properties were 2–3 times shorter than in the previous case. It was found in both cases that modes of loading involving compressive stress were more adversely affected by fire exposure than those involving tension.

A simple ‘two-layer’ model is proposed, in which the laminate is assumed to comprise (i) an unaffected layer with virgin properties and (ii) a heat-affected layer with zero properties. For residual properties after fire, the ‘effective’ thickness of undamaged laminate was calculated using this model and compared with measured values. A thermal model was employed to predict the temperature and the residual resin profile through the laminate versus time. Comparing the model predictions with the measured values of effective laminate thickness enabled simple criteria to be developed for determining the position of the ‘boundary’ between heat-affected and undamaged material. For post-fire integrity of unloaded laminates, this boundary corresponds to a Residual Resin Content (RRC) of 80%, a criterion that applies to all the resin types tested.

*Author to whom correspondence should be addressed.

For polyester laminate under load in fire, the boundary in compressive loading (buckling failure) appears to correspond to the point where the resin reaches 170°C. In tensile loading, significant strength is retained, because of the residual strength of the glass reinforcement.

The model was used to produce predictions for 'generic' composite laminates in fire.

KEY WORDS: Author please supply Keywords ???

INTRODUCTION

PREDICTIVE TOOLS FOR the fire response of composites are required for most structural applications. This paper describes the results of a collaboration between two research teams, and proposes simple criteria for the loss of load-bearing capability in two important situations: (i) residual properties of unloaded laminates damaged by fire, and (ii) failure of laminates under load during fire exposure.

Most transport applications involve regulations on fire performance that vary between industries [1–6]. Composites with resins based on solvent monomers such as styrene usually have short ignition times, high heat release rates and may produce smoke and toxic products. Various means are used to mitigate these effects [7], including the incorporation of halogens to suppress ignition, phosphorus additives to promote char formation, and antimony compounds, that interfere with the combustion reaction. Improvements in one property, however, such as ignitability, are usually accompanied by adverse effects on others, such as toxic product generation or reduced mechanical properties.

Although the load-bearing capability of unprotected composite structures is known to be severely degraded by fire [8–16], there is limited understanding of the factors that influence this. DSTO and RMIT subjected several types of laminate to controlled heat flux and measured the residual properties at room temperature [13–16]. These properties could be related to the depth of char using a simple 'two-layer' mechanical model in which the components were assumed to be (i) undamaged laminate with virgin properties and (ii) residual char with considerably lower values of modulus and strength.

The Newcastle group developed a thermal model for the decomposition of composite laminates in fire [17–19]. The model predicts the evolution of the temperature and resin content in the laminate with time for any surface conditions. It takes account of heat transport by conduction through the laminate, the effect of resin decomposition, which is an endothermic process, and the cooling effect of volatile resin decomposition products passing through the laminate. Application of the model requires knowledge of the decomposition process of the resin, which can generally be acquired through thermogravimetric analysis (TGA).

In a previous joint publication [20] it was shown that by combining the Newcastle thermal model with the two-layer model of Mouritz et al. [13–16], the residual post-fire mechanical properties could be calculated with reasonable accuracy. The present paper extends the previous work to explore the possibility of modelling fire behaviour under load. We again employ the thermal model in conjunction with the two-layer mechanical model to determine criteria for the 'boundary' between heat-affected and undamaged laminate.

EXPERIMENTAL

Materials

Three generic types of glass fibre composite were used. These were based on polyester, vinyl ester and phenolic resin. Most of the material details have been given elsewhere [13–16]. For the additional work on laminates under load an isophthalic polyester resin was supplied by Reichold and the woven glass reinforcement by Owens Corning Fibreglass. The laminates were reinforced with an E-glass woven fabric and fabricated by hand lay-up. The polyester and vinyl ester laminates were allowed to post-cure at room temperature for several weeks prior to fire testing. We acknowledge that the cure level of these laminates will have been somewhat lower than that of laminates post-cured at elevated temperature. However, this is typical practice when manufacturing large marine structures from these resins. The fibre volume fraction was 0.35.

The phenolic laminates were cured at room temperature for 24 h, followed by a post-cure at 60°C for 1 h and 80°C for 2 h. The fully cured phenolic laminate had a fibre volume fraction of 0.39. All the laminate specimens were nominally 12.0 mm thick.

Unloaded Samples

A known one-sided heat flux was applied to 12 mm thick laminate samples. In the first set of measurements, on laminates without load present, the conical radiative heating element of a cone calorimeter [13–16,20] was used, as shown in Figure 1. The cold face of the specimens was thermally insulated. The applied heat flux (25–100 kW/m²) resulted in a rapid surface temperature rise (e.g. to approximately 650°C at a heat flux of 50 kW/m²).

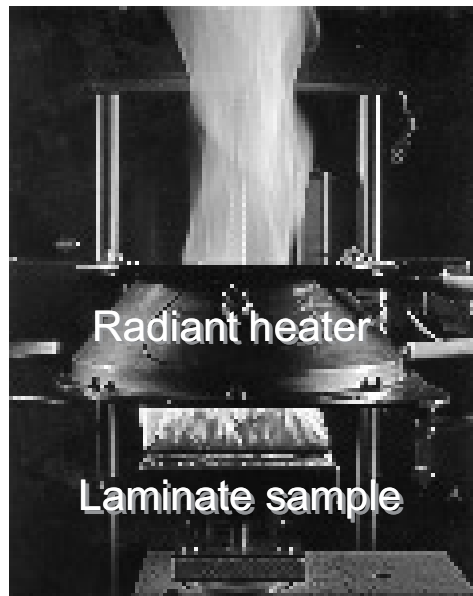


Figure 1. Exposure of composite laminate to a reproducible heat flux using a cone calorimeter.

There is therefore an induction period, the ignition time, before there are sufficient flammable decomposition products to permit ignition. Following this, the process of ‘flashover’ occurs, in which flames spread across the entire surface.

At 50 kW m^{-2} the polyester laminates ignited after about 30 s and the phenolics considerably later, after 460 s. Following ignition, the combustion process led to progressive resin depletion and char formation. After a measured period of exposure, the samples were extinguished and cooled to room temperature for mechanical measurements. The char layer thickness was measured from micrographs of the sections. The results reported here relate mainly to polyester and phenolic, but vinyl ester laminates behaved in a very similar manner to the polyester ones.

Figure 2 shows a typical section after fire exposure, and a sketch of the change in residual matrix content through it. There are three regions: undamaged laminate, damaged laminate (in which there is progressive resin decomposition) and residual char. It is interesting to note that the early part of the decomposition zone is characterised by the presence of a number of small delaminations. These were probably caused by the pressure of volatile products acting within laminate in which the resin had been weakened by temperature and decomposition. Their effect on heat flow and properties has not been taken into account in the modelling presented here. The decomposition zone extends for a few millimetres, so visual determination of the ‘effective’ boundary between damaged and undamaged material is somewhat subjective and can be subject to scatter, of typically about $\pm 1 \text{ mm}$ in a 12-mm laminate.

Figure 3 shows scanning electron micrographs of the structure of the char within (a) polyester and (b) phenolic laminates. The char region in the glass–polyester is largely depleted of resin, leaving mainly exposed fibres. The vinyl ester laminates showed very

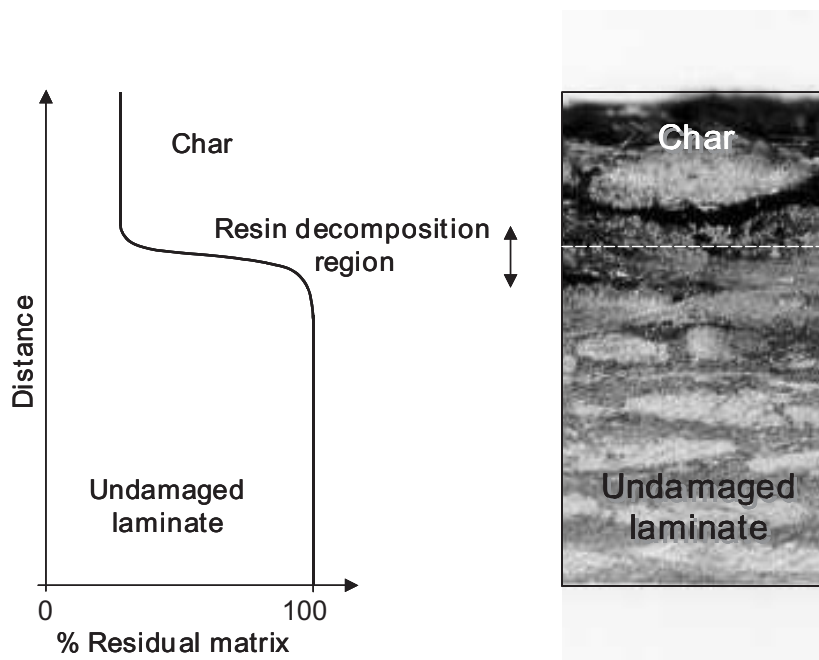


Figure 2. Schematic of resin degradation through laminate, with resin decomposition zone and residual char, alongside a cross-section through a glass/polyester woven roving laminate exposed to a heat flux of 50 kW/m^2 .

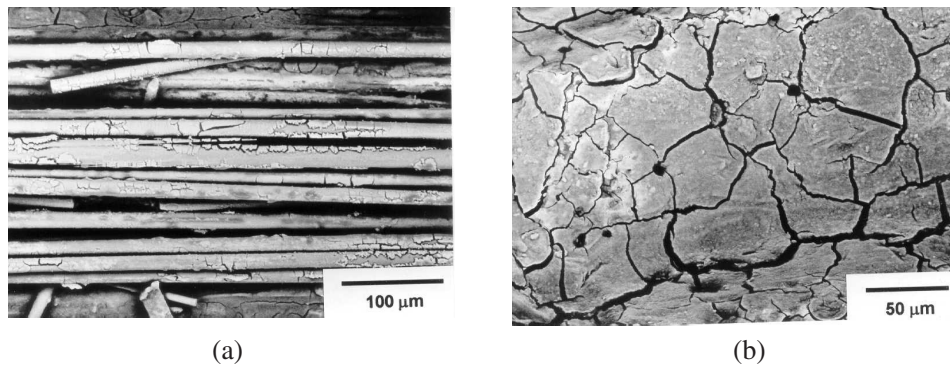


Figure 3. Scanning electron micrographs showing the microstructure of char in (a) glass–polyester and (b) glass–phenolic laminates. The char observed in glass–vinyl ester laminates is very similar to that in (a).

similar behaviour. By contrast, the glass–phenolic can be seen to contain a substantial residue of heavily cracked carbonaceous char. In addition to the cracks, holes can also be seen, originating presumably from voids formed during cure.

The post-fire tension, compression and flexural properties of the laminates were determined at 20°C, at least four specimens being tested for each reported property value.

The tensile stiffness and strength were measured according to ASTM tensile test specifications [21] using coupons with 100 mm gauge length and 25 mm width. Tensile ‘stiffness’ (in N/m) was determined instead of Young’s modulus because of the difficulty of measuring strain on a fire-damaged laminate. The stiffness was determined from the gradient of the linear portion of the load/displacement curve.

Compression tests were performed on slender composite beams, 150 mm long and 25 mm wide, simply supported. The compression stiffness was again determined as the slope of the load/displacement curve. The Euler buckling strength was taken to be the applied stress at which the specimen began to buckle. Compression tests were only performed on the glass–polyester laminate.

Flexural modulus and strength were determined using the ASTM four-point bend method [22]. The specimens were 240 mm long, 25 mm wide, and were loaded at a crosshead speed of 5 mm/min in quarter-point loading, with the fire-damaged surface in compression.

Loaded Samples

In the second series of experiments, measurements were carried out on laminates loaded in tension and in compression during fire. For these experiments, which involved only 10 mm thick polyester laminates with the rear face insulated, a calibrated propane burner, as shown in Figure 4, replaced the electric cone. During the test, the temperature at a point 10 mm in front of the hot face of the laminate was maintained at 800°C by adjusting the burner flame. In calibration experiments with a copper slug heat flux meter [23], it was found that this condition gave a reproducible heat flux of 75 kW m^{-2} at the laminate surface. It is therefore reasonable to assume that this condition produces a similar thermal insult to the cone calorimeter element used previously. Similar ignition

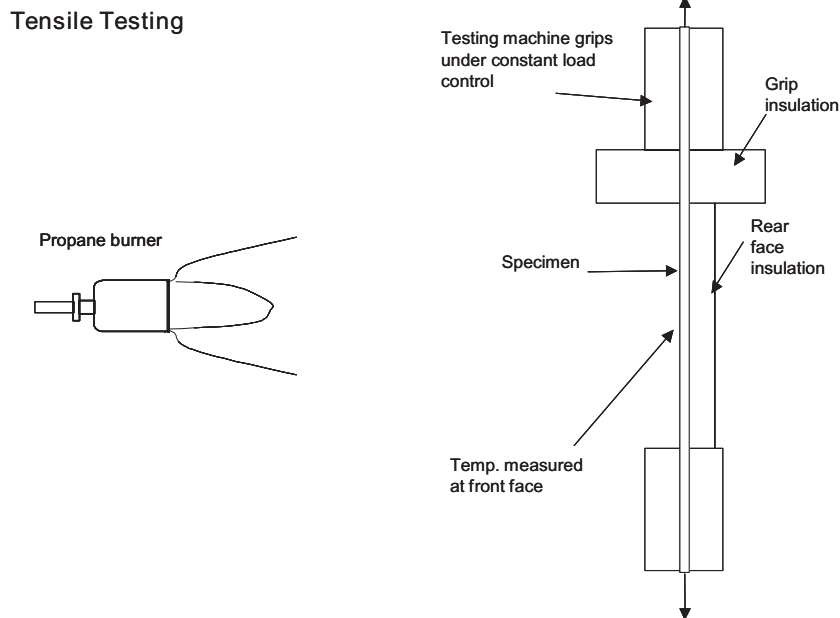


Figure 4. Experimental set-up for fire exposure under tensile load using a calibrated propane burner.

times of about 10 s were found for polyester laminates in both types of test, which supports this assumption.

A constant vertical load was applied to the samples with a testing machine, which was insulated using kaowool. Fume extraction was provided. All samples tested were 10 mm thick by 100 mm wide. This enabled a region 100 mm square to be exposed to the heat flux. For the tensile loading, 40 mm long samples were loaded using the wedge grips of the testing machine. In this mode it was necessary to insulate the upper grip with about 15 mm thick kaowool to prevent it from overheating, and resulting in premature grip slippage.

For compressive loading, two types of test were carried out. Initially, 150 mm long samples were simply supported, as in the previously reported compression tests. Global Euler buckling limited the compressive stress that could be applied to these samples. In order to achieve higher compressive stresses, nearer to the design stresses that might be used in some composite structures, additional constraint was provided to delay the onset of buckling. It was found that an excellent way of accomplishing this, while still allowing a substantial region of the specimen to be subjected to heat flux, was to use a test jig with anti-buckling guides similar to the well-known Boeing compression test [24], but with a square, rather than rectangular sample. The set-up is shown in Figure 5.

Thermogravimetric Analysis

The thermal model requires knowledge of the decomposition reaction in the resin. This is generally most conveniently acquired by TGA. The resin decomposition parameters were determined from the TGA curves at a heating rate of 25°C/min in nitrogen, and given in Figure 6. The polyester and vinyl ester have very similar curves: both resins begin

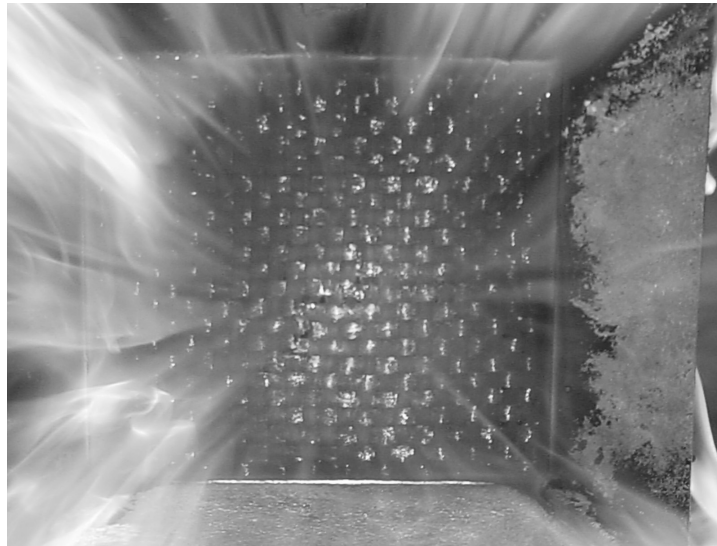
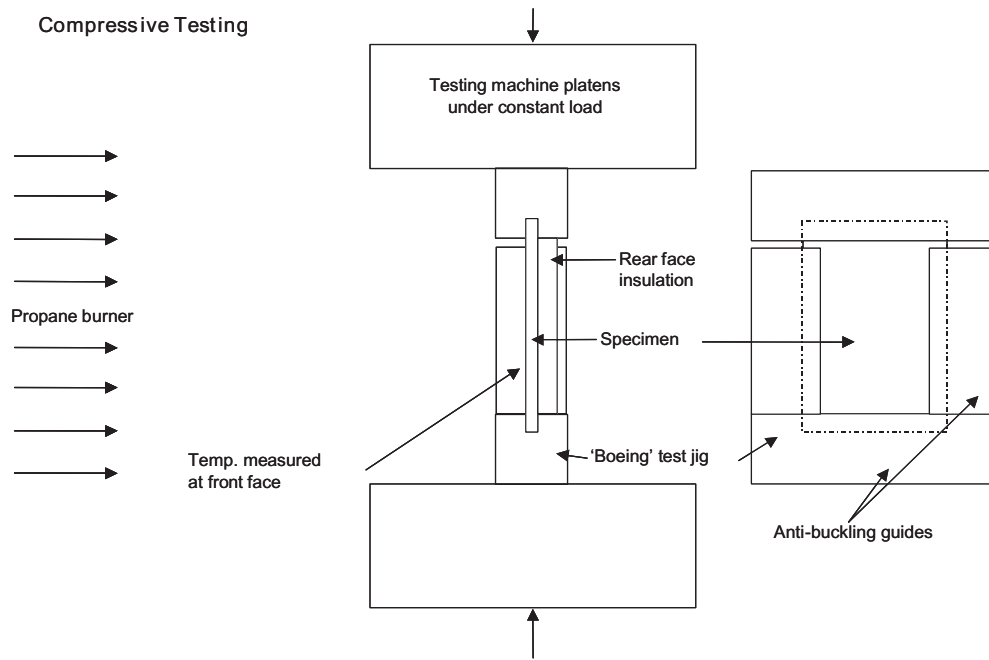


Figure 5. Above: experimental set-up for fire exposure under constrained compressive load using a calibrated propane burner. Below: sample under test.

to decompose at 350°C and the reaction is substantially complete at 480°C, leaving less than 7% of the initial mass as a carbonaceous char. Phenolic resin, which has a higher aromatic content, leaves a larger proportion of char, as observed in Figure 3(b). The thermal response of the phenolic is preferably modelled by a two-stage reaction to account for primary condensation followed by char formation [18,20].

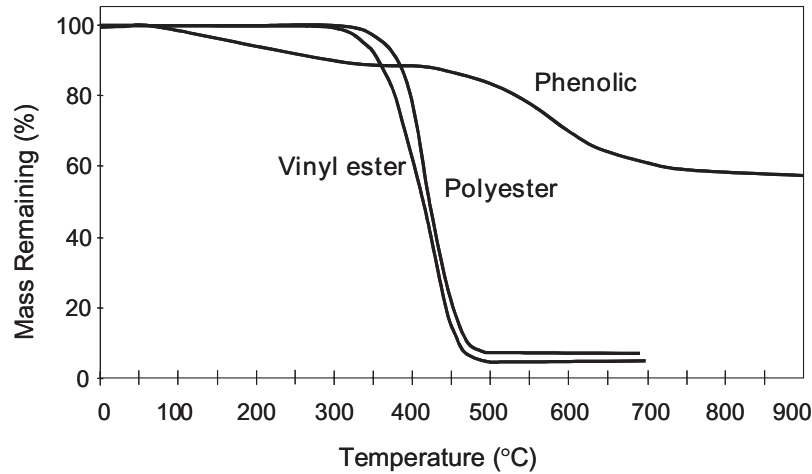


Figure 6. TGA curves at 25°C/min for isophthalic polyester, vinyl ester and phenolic resins in a nitrogen atmosphere.

THERMO-MECHANICAL MODEL

The ‘two-layer’ approach to modelling the behaviour of laminates during or after fire consists of two analysis steps. The first is the use of the thermal model to predict the profile of the temperature and resin content through the thickness. Following this, the two-layer model is used to describe mechanical behaviour both during and after the fire.

Thermal Model

There are several published models for the decomposition of organic materials in a fire, including wood, ablative re-entry protection materials, and composites [25–33]. Gibson and colleagues used a thermal model of this type to predict the decomposition of polymer composites in fire [17–20]. The model predicts the evolution of temperature and reduction in resin content of a laminate with time for any surface boundary condition.

As mentioned in the previous section, in addition to the process of conduction there are two other phenomena which can affect the energy transfer through composite laminates in fire: the decomposition of the matrix phase, which is highly endothermic, and the flow of volatile products from the decomposition region towards the hot face. These effects can be incorporated into a model for the thermal response by including terms for the energy fluxes due to decomposition and mass flow in the unsteady state heat conduction equation:

$$\frac{\partial}{\partial x} \left(k \frac{\partial T}{\partial x} \right) + \dot{q} = \rho c_p \frac{\partial T}{\partial t} \quad (1)$$

For polyester and vinyl ester resins the endothermic decomposition can be described by a single thermally activated process:

$$\frac{\partial m}{\partial t} = -A \left[\frac{(m - m_f)}{m_0} \right]^n e^{(-E/RT)} \quad (2)$$

where m , t and T are the mass, time and temperature variables respectively, A , E and n are the rate constant, activation energy and order of the reaction and R is the gas constant.

Assuming thermal equilibrium between the decomposing laminate and the resultant gases, the enthalpy and mass flux of the reaction products define the energy flux due to mass transfer. The magnitude of the mass flux of decomposition products is known from the reaction kinetics and these products can be assumed to flow through the damaged material towards the fire, the undamaged material being impermeable. Generation of delamination cracks and their consequences are not considered, although they are known to occur. The full governing equation is therefore:

$$\rho C_P \frac{\partial T}{\partial t} = \frac{\partial}{\partial x} \left(k \frac{\partial T}{\partial x} \right) - \dot{M}_G \frac{\partial}{\partial x} h_G - \rho A \left[\frac{(m - m_f)}{m_0} \right]^n e^{-(E/RT)} (Q_P + h_C - h_G) \quad (3)$$

where T , t and x are temperature, time and through-thickness coordinates, respectively. ρ , C_P and k are the density, specific heat and conductivity of the laminate. \dot{M}_G is the mass flux. h_C and h_G are the respective enthalpies of the composite and evolved gas. Q_P is the endothermic decomposition energy. The three terms on the right hand side relate to heat conduction, volatile convection and the decomposition endotherm, respectively.

A finite difference version of the thermal model has been validated for different resin systems by comparing the calculated and measured thermal responses during furnace fire tests [17,18]. The modelling parameters for this have been reported previously [18]. A finite element-based model has also been developed and reported [19].

The boundary conditions for the application of the model were an incident hot surface heat flux of 50 or 75 kW/m², as appropriate, with a surface emissivity of 0.8. The cold face was assumed to be fully insulated.

Two-layer Model

Mouritz and Mathys [13–15] proposed the two-layer model to estimate residual mechanical properties after fire. Here it will be used to interpret behaviour both during and after fire.

The model assumes the laminate to consist of two layers:

- (i) a thermally affected region with reduced (or zero) mechanical properties.
- (ii) an undamaged region containing unaffected virgin material with room temperature mechanical properties.

In relation to residual properties after fire we previously referred to these regions as the ‘char region’ and the ‘unburnt region’ [13–16,23], and it was shown that the thickness of the former was closely related to that of the thermally damaged material observed optically, as in Figure 1. In the residual property case the char region contained visibly damaged material where the resin content had clearly been depleted by decomposition. It was suggested that the criterion for the position of the ‘effective’ boundary between the two layers should be a particular level of RRC.

We now wish to extend this concept to attempt to model behaviour under load during fire – hence the change in nomenclature from ‘char’ region to ‘thermally affected’ region. It will be shown here that the period of fire integrity is considerably reduced when the

laminates is under load, so we can expect the criterion for the boundary between the two regions will be different.

The underlying assumption of the model is that the properties of the two regions can be combined as if they were a two-layer laminate. Hence, the stiffness, S , in tension or compression can be estimated using the simple expression:

$$S = \left(\frac{d - d_t}{d} \right) \cdot S_0 + \left(\frac{d_t}{d} \right) \cdot S_t \quad (4)$$

where d_t is the thickness of the thermally affected region, d is the original thickness of the laminate, and S_t and S_0 respectively are the stiffnesses of the affected and unaffected material.

Similarly, the tensile or compressive strength can be determined by:

$$\sigma = \left(\frac{d - d_t}{d} \right) \cdot \sigma_0 + \left(\frac{d_t}{d} \right) \cdot \sigma'_t \quad (5)$$

where σ_0 is the tensile or compressive strength of the unaffected material, and σ'_t is the stress in the affected material at the failure strain of the unaffected material.

We now approximate the flexural stiffness, or more precisely the ' EF ', value of a laminate as $\bar{E}_0 b (d - d_t)^3 / 12$, where \bar{E}_0 is the flexural modulus of the unaffected material. The Euler buckling load for a plate, breadth, b , and height, L , is therefore

$$P_c = \frac{C \pi^2 \bar{E}_0 b (d - d_t)^3}{12 L^2} \quad (6)$$

where the constant, C , should be close to unity for pin-jointed loading at both ends. The apparent stress at which buckling occurs, which of course is based on the original (undamaged) thickness of the laminate, will be

$$\sigma_c = \frac{C \pi^2 \bar{E}_0 (d - d_t)^3}{12 d L^2} \quad (7)$$

Because of the cubic nature of the term in residual thickness it can be expected that fire will have the most severe effect in loading modes involving buckling. In the present study, some constrained compression measurements were also carried out, in order to achieve higher compressive stresses than in the Euler case. For this work a rig with roughly similar geometry to the Boeing compression test [34] was employed. The loading mode in this case resembled a plate supported on all four sides, so that the collapse load is given [26] by an expression of the form

$$P_c = \frac{C' \bar{E}_0 (d - d_t)^3}{b} \quad (8)$$

Here, the constant, C' , depends both on the length-to-breadth ratio, L/b , and on the nature of the constraint offered by the loading jig. For an approximately square plate, C' varies according to laminate properties and how the plate is supported [34–36].

The apparent collapse stress for this case, again based on original (undamaged) thickness is

$$\sigma_c = \frac{C' \bar{E}_0 (d - d_f)^3}{b^2 d} \quad (9)$$

In this situation failure is due to elastic instability in the form of local buckling in the heated region of the sample as opposed to global buckling. In this paper all compressive collapse will be assumed to result from elastic instability. When the level of fire damage is low, the failure mode may well involve true compressive failure, rather than buckling, depending on the plate dimensions and the modulus of the laminate. The transition between the two failure modes through fire damage forms the basis of an ongoing study. It can be expected that as damage progresses in this test local buckling will tend to quickly take over from compressive failure. This is evident from the cubic effect of the residual thickness term in Equation (9), as opposed to its linear dependence in Equation (5), which determines compressive failure.

In contrast to flexural stiffness and buckling resistance, the apparent flexural strength is proportional to the section thickness squared and can be taken as proportional to $(d - d_f)^2$. The appealing feature of the two-layer model can be seen to be the simplicity of the analysis.

RESULTS AND DISCUSSION

Unloaded Samples: Residual Integrity

Figure 7 shows the experimental relationship between measured char thickness and heating time for polyester laminates at a heat flux of 50 kW m^{-2} . As discussed above, there is some vertical scatter on these points because of the difficulty in determining the position of the centre of the decomposition region. It was decided to investigate whether the effective boundary between damaged and undamaged material could be simply approximated in terms of a stipulated residual resin content (RRC) in the laminate.

The thermal model (continuous curves) was used to calculate the times at which the laminate reached a stipulated RRC at different points through its thickness. Curves of damage depth vs. time were modelled for a range of RRCs between 30 and 98%. The model can be 'calibrated' by comparing the experimental and model values in Figure 7. It can be seen that, over the full range of thickness, agreement is closest for an RRC of 80%. This implies that the resin (once cooled to room temperature) ceases to contribute significantly to mechanical behaviour once 20% of it has been volatilised. Of course the residual char does possess a certain level of mechanical strength and stiffness, but these values are very low compared with those of the undamaged laminate.

Figure 8 shows thermal damage depth after a fixed period of 325 s for a range of heat flux values. Again the RRC 80% criterion can be seen to apply across the range. It is interesting to note that the rate of material loss varies in a less than linear manner with increasing heat flux: being approximately proportional to heat flux to the power 0.7.

Surprisingly, a similar optimum RRC of 80% was also found from the results of similar modelling on the phenolic laminates, shown in Figure 9. Here RRC values of 75–98%

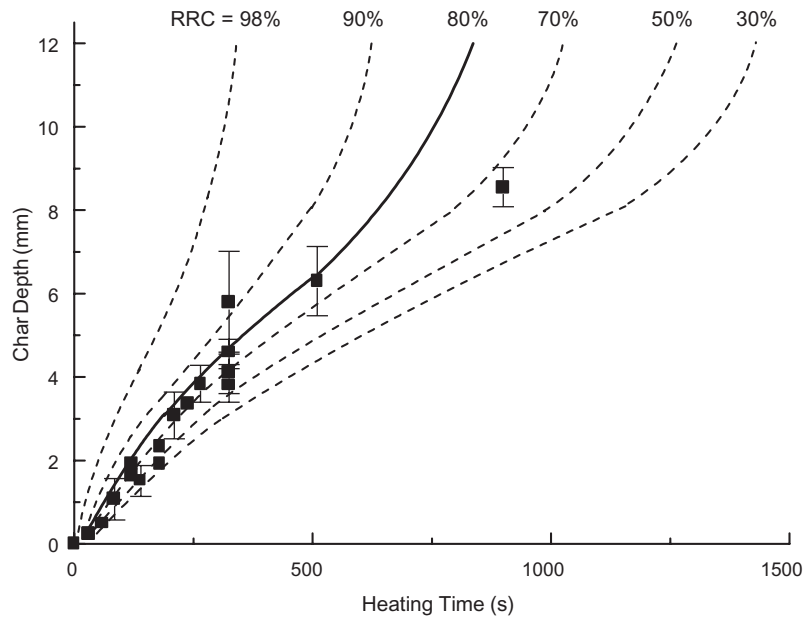


Figure 7. Thermal damage depth vs. heating time for a heat flux of 50 kW/m^2 , for 12-mm thick glass–polyester laminates. The curves show the RRC at the interface between the char and undamaged laminate determined using the thermal model, for RRC values in the range 30–98%.

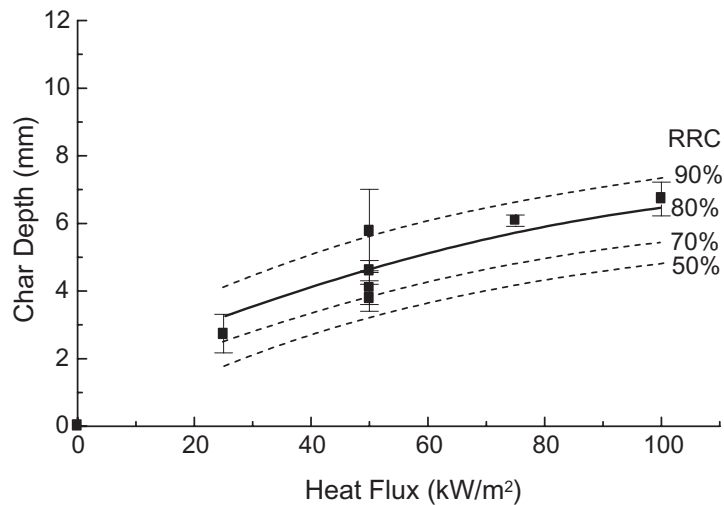


Figure 8. Effect of heat flux on char thickness for a heating time of 325 s for glass–polyester laminates. The curves show the RRC at the interface between the char and undamaged laminate determined using the thermal model.

were used. It is interesting to note from Figure 6 that an RRC of 80% appears to coincide approximately with the end of the first stage of the phenolic reaction. Phenolic char formation may play less of a role in the materials investigated here, from a mechanical viewpoint, than might have been expected.

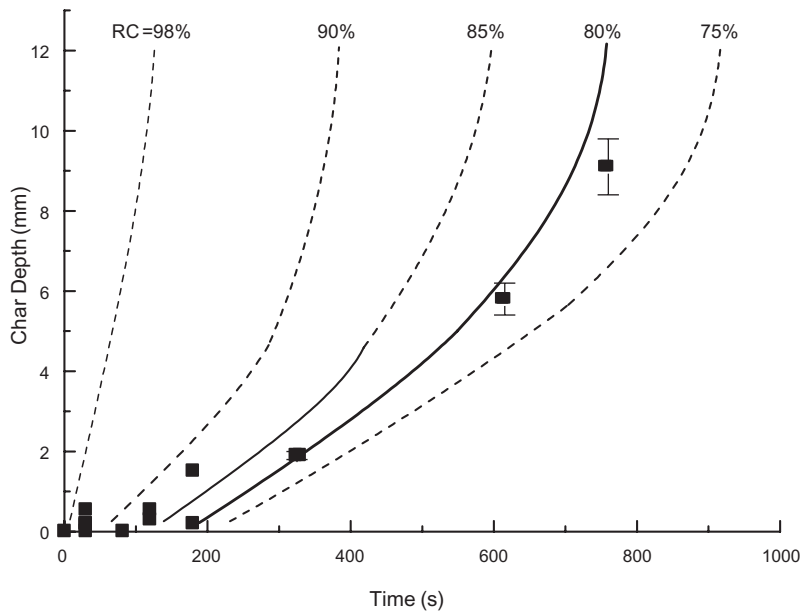


Figure 9. Thermal damage depth vs. heating time for a heat flux of 50 kW/m^2 for 12-mm thick glass-phenolic laminates. The curves show the RRC at the interface between the char and undamaged laminate, determined using the thermal model, for RRC values in the range 75–98%.

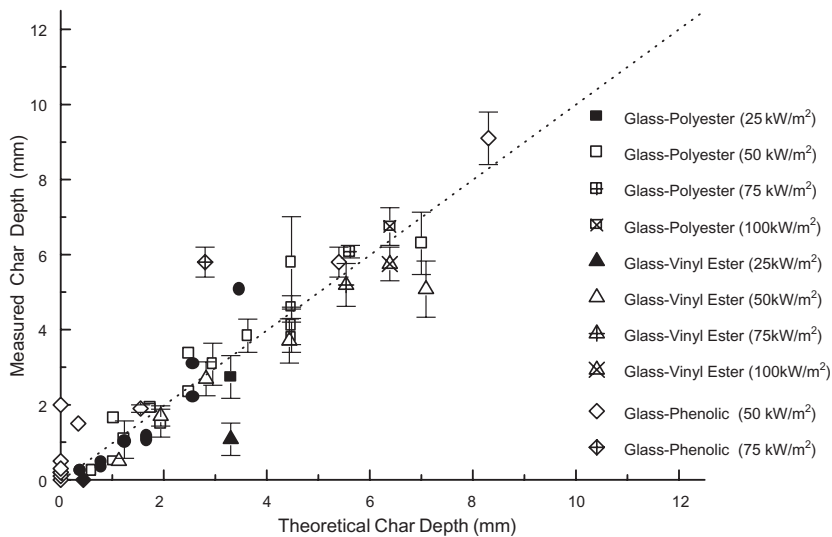


Figure 10. Comparison of the theoretical char depth, determined using the thermal model with char thickness values measured by microscopy, for all the laminate types studied at heat fluxes in the range 25–100 kW/m^2 .

Figure 10 shows a comparison of the theoretical char depth determined using the thermal model for all the laminate types studied at heat fluxes in the range 25–100 kW/m^2 . Even allowing for a significant degree of scatter in the char depth determination it can be seen that agreement is quite encouraging.

The predicted relationship between ‘char’ depth and time, for an RRC of 80% was then used in the simple two-layer formulae [14,15] to calculate residual tensile and flexural properties. The predictions are compared with the experimental results for the residual tensile properties of polyester and vinyl ester laminates in Figures 11 and 12. Both resin types show very similar behaviour and it can be seen that there is excellent agreement between model and experiment for both residual stiffness and strength. The discontinuity in the model curves occurs when all the material through the thickness of the laminate has reached the stipulated RRC of 80%. At this point, all the material is assumed to consist of the char phase.

Figure 13 shows a similar comparison for phenolic laminates. Again, agreement is very good. It is interesting to note, on comparing the phenolics with the polyester and vinyl ester, that both the model and the results underline the very different decomposition characteristics of the two classes of resin. In the polyester, resin loss begins at a relatively low temperature and continues progressively. With the phenolic, there is a delay before resin loss begins, but once this commences the property loss is more rapid than in the polyester case. This reflects the different activation energies for the decomposition process in the two polymers [18].

Figures 14 and 15 compare the results for flexural modulus and flexural strength for the polyester laminates. These results can be expected to be more sensitive to modelling errors because, as mentioned previously, the measured flexural modulus and strength are a function, respectively, of the cube and the square of the undamaged laminate thickness. Agreement for the modulus values is again very good, and for the strength values, moderate.

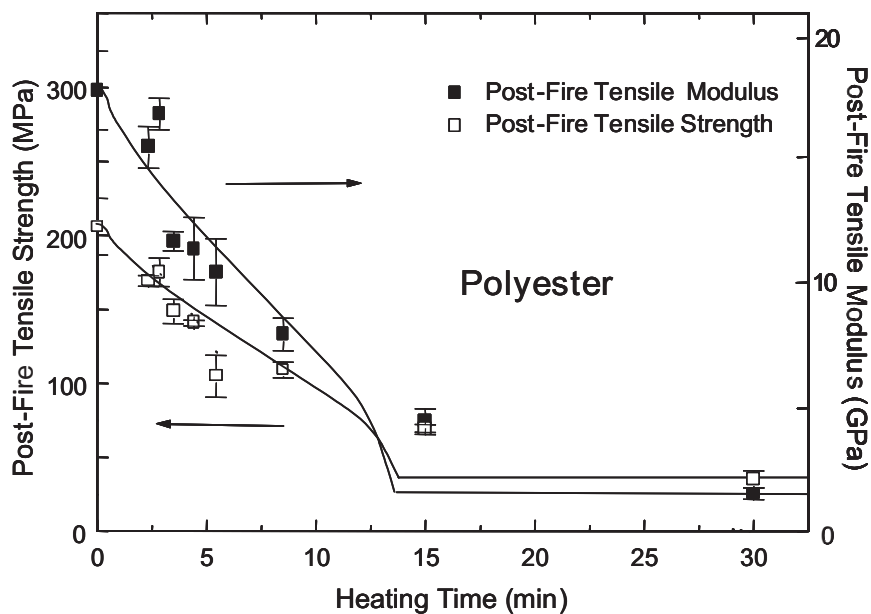


Figure 11. Change in residual tensile properties of glass–polyester laminate with heating time at a heat flux of 50 kW/m^2 (experimental points). The curves show the theoretical post-fire properties determined using the two-layer model.

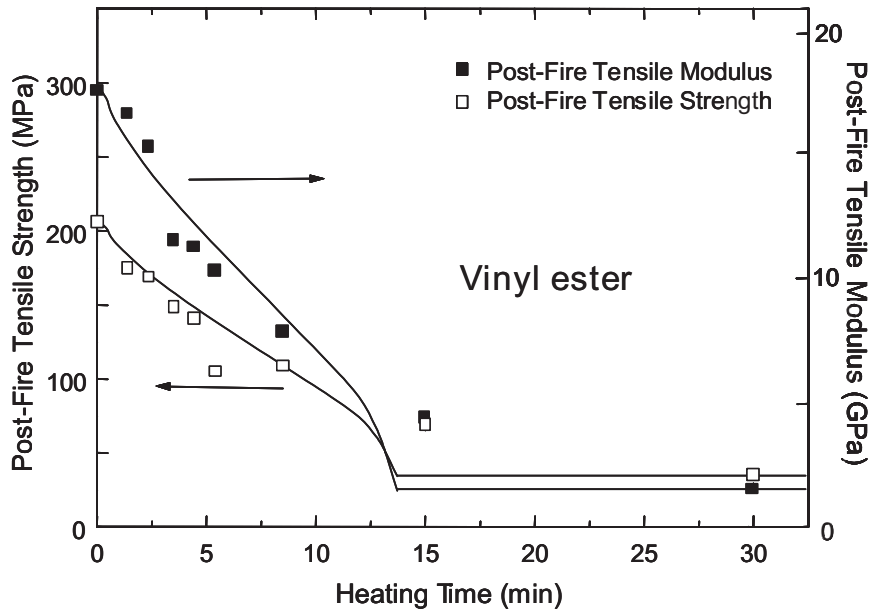


Figure 12. Change in residual tensile properties of glass-vinyl ester laminate with heating time at a heat flux of 50 kW/m^2 (experimental points). The curves show the theoretical post-fire properties determined using the two-layer model.

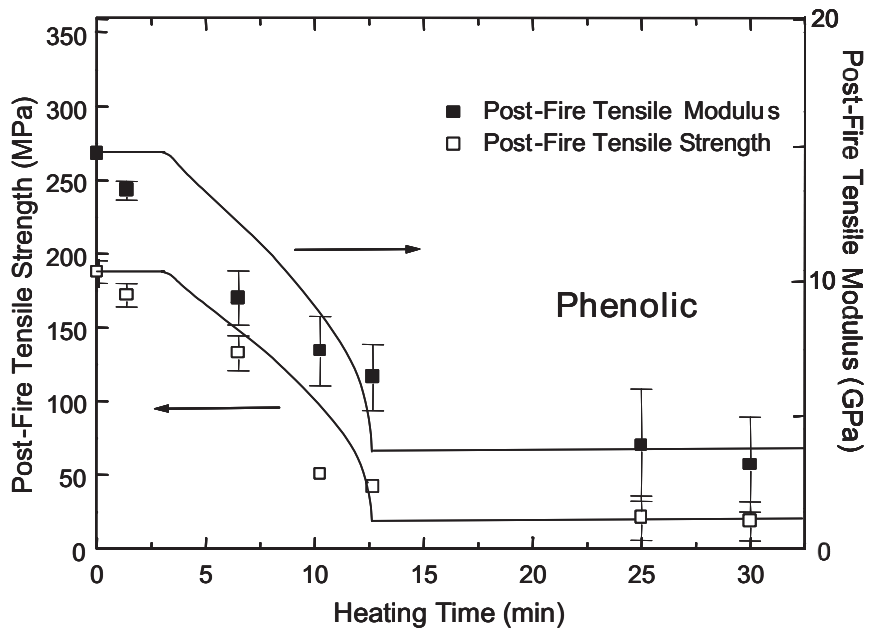


Figure 13. Change in residual flexural properties of glass-phenolic laminate with heating time at a heat flux of 50 kW/m^2 (experimental points). The curves show the theoretical post-fire properties determined using the two-layer model.

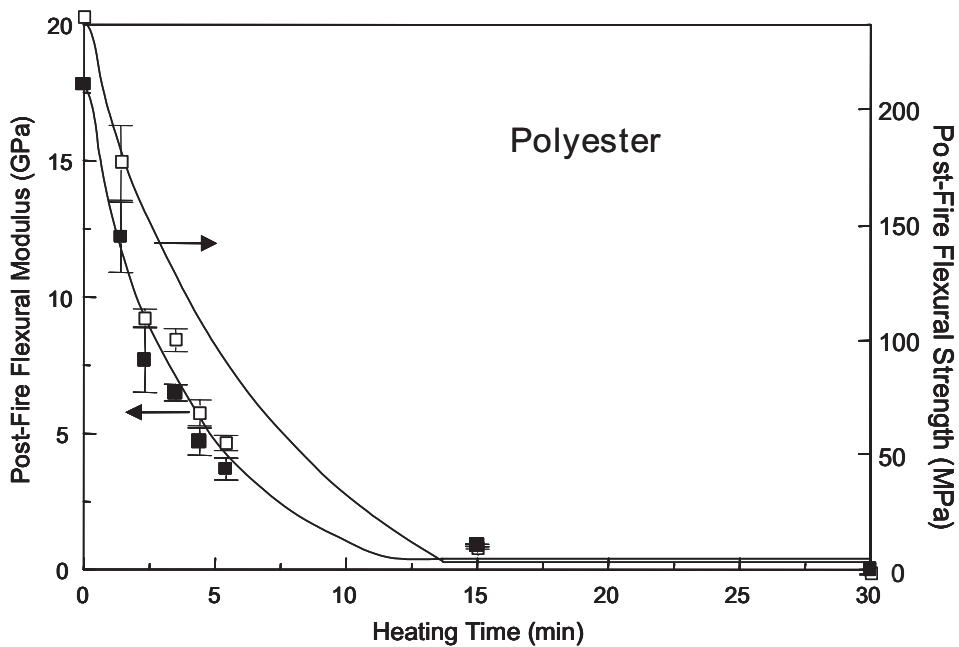


Figure 14. Change in residual flexural properties of glass-polyester laminate with heating time at a heat flux of 50 kW/m^2 (experimental points). The curves show the theoretical post-fire properties determined using the two-layer model.

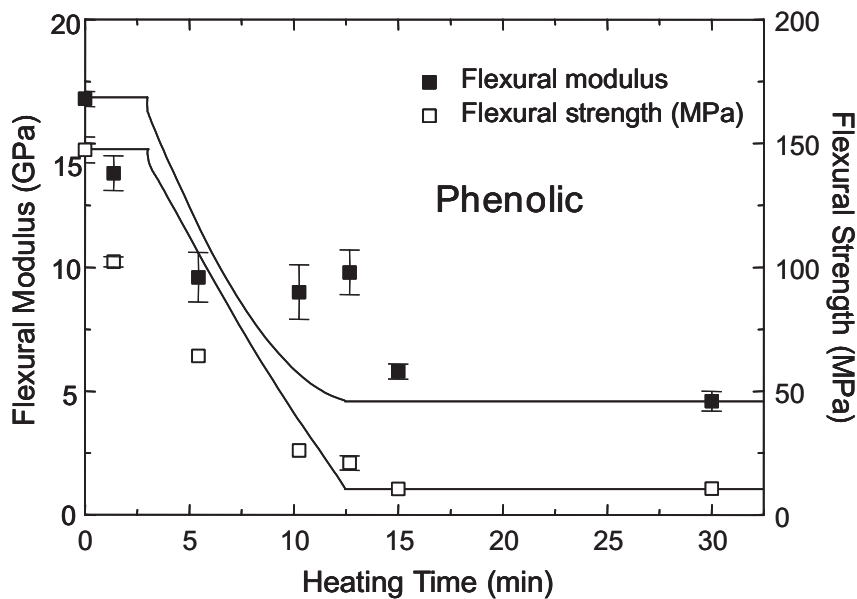


Figure 15. Change in residual flexural properties of glass-phenolic laminate with heating time at a heat flux of 50 kW/m^2 (experimental points). The curves show the theoretical post-fire properties determined using the two-layer model.

Integrity of Loaded Samples in Fire

Figure 16 shows the results obtained from the burner tests under tensile and compressive loading. The onset of failure at a particular time was, in all cases, characterised by a clear loss of load-bearing capability that took place over just a few seconds. It can be seen that the integrity times under load are considerably shorter than those for the residual properties. In addition, the integrity times under load are much shorter than those observed for the unloaded samples. The samples under compressive load in particular were very strongly affected. In tension, where behaviour can be expected to be strongly influenced by the strength of the reinforcement, the effect of load is a little less severe and samples survive for reasonably long times at a significant proportion of their static failure stress.

The aim of the tests under load was to generate measurements at stresses typical of design stresses in composite structures – i.e. approximately 1/4 of the static strength at room temperature. In the polyester laminates the room temperature tensile and compressive strength values were both about 210 MPa, implying that stresses of the order of 52.5 MPa would be desirable. This was achieved easily in the case of the tensile measurements, but was not possible in the Euler tests because global buckling intervened at relatively low values of compressive stress. It was for this reason that the constrained compression ('Boeing') tests were carried out. In these experiments higher stresses, typical of the compressive stresses in parts of a well-designed structure, were achieved, as can be seen from Figure 16. Failure in the constrained tests still took place by buckling (local, as opposed to global), as discussed in the next paragraph underlining that this is a dominant

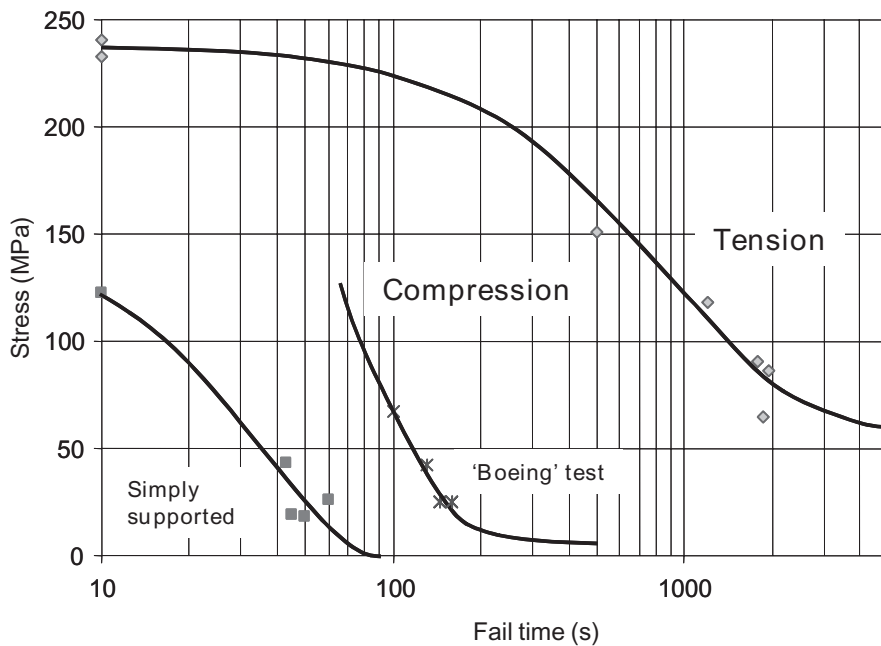


Figure 16. Relationship between stress and failure time for 10-mm polyester laminates, subject to 75 kW/m^2 in burner test. Upper curve shows the results for tensile loading, middle curve shows compressive stress (Boeing compression jig, $W/d = 10$), lower curve is compressive stress (Euler buckling, $b/d = 15$).

failure mode for many composite structures in fire. It is interesting to note that Figure 16 is presented with a format similar to that used for environmental or stress rupture tests, albeit with much shorter times. We believe that the most appropriate practical way forward for characterising the fire behaviour of composite parts under load is to use the characterisation approach adopted here, which will allow failure times under load to be found from the curve by interpolation or extrapolation.

Figure 17 shows values of the heat-affected layer thickness calculated from the buckling results shown in Figure 16. From Equations (6) and (8) it can be seen that d_t at a particular failure time can be found from the ratio of the test load to the failure load in a short-term test at room temperature, so

$$\frac{P_c}{P_{c_0}} = \left(\frac{d - d_t}{d} \right)^3 \quad (10)$$

Hence d_t can be found from

$$d_t = d \left(1 - \sqrt[3]{\frac{P_c}{P_{c_0}}} \right) \quad (11)$$

In the case of the Euler buckling measurements it was possible to measure the room temperature failure load, P_{c_0} , directly. For the constrained experiments, failure at room temperature occurred by compressive failure, rather than global buckling, so it was necessary to calculate the room temperature buckling stress from Equation (10). The calculated d_t values were used in Equation (5) to check on the possibility of compressive failure,

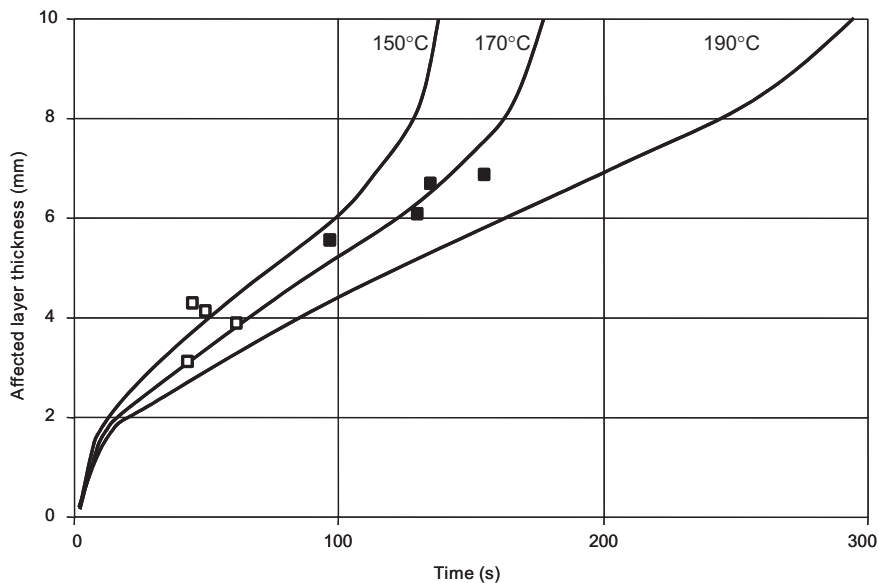


Figure 17. Relationship between thickness of heat-affected layer and time for 10-mm polyester laminates, subject to compressive loading and 75 kW/m^2 heat flux. Experimental points are derived from the results shown in Figure 16. Open symbols: Euler buckling. Closed symbols: local buckling in the 'Boeing' test. Curves are from thermal model, assuming property loss to occur at 150, 170 and 190°C.

but this was not shown to have occurred in any of the fire tests under load. Of course compressive failure would be possible in this type of test, at higher stresses and shorter failure times. Indeed at some point one may expect a transition between compressive failure and local buckling, but this transition was not investigated in the present study.

In arriving at a criterion for determining the value of d_t from the fire model, it was borne in mind that failure occurs at much shorter times than in the case of the residual strength modelling discussed previously. Indeed in some cases the failure times may be so short that relatively little permanent decomposition damage will have occurred prior to sample collapse. It was therefore considered that the RRC criterion used previously for residual strength would probably not be suitable. Instead, a ‘temperature’ criterion was investigated. As shown from the calculated curves in Figure 17, it was assumed that complete loss of compressive stiffness occurred at a particular temperature. The figure shows predictions for a number of temperatures, but it is clear that the value of 170°C calibrates well with the results found so far on polyester composites. It is important to note that this does not correspond to an isothermal temperature at which the material loses significant compressive mechanical properties but instead has been found to provide a useful calibration when modelling the effect of a dynamic temperature gradient on the mechanical response.

Figure 18 shows a similar attempt to model the tensile strength behaviour. In this case, due to the form of Equation (5), the residual thickness was assumed to be directly proportional to the reduction in strength, so

$$d_t = d \left(1 - \frac{P_T}{P_{T_0}} \right) \quad (12)$$

where P_{T_0} and P_T are the tensile failure loads prior to and during fire exposure.

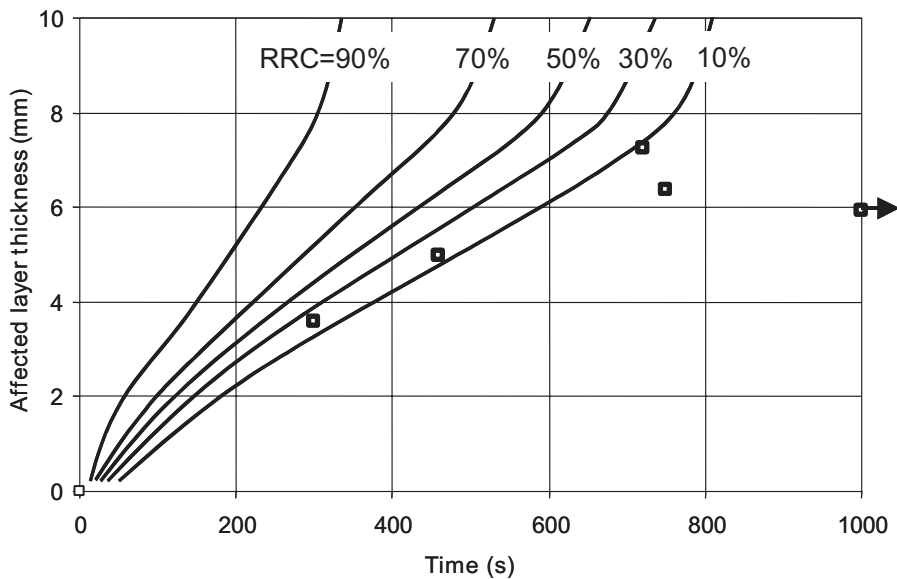


Figure 18. Relationship between thickness of heat-affected layer and time for 10-mm polyester laminates, subject to tensile loading and 75 kW/m^2 . Experimental points are derived from the results shown in Figure 16. Curves are calculated from thermal model, assuming property loss to occur at RRC of 90, 70, 50, 30 and 10%.

Because the retention times were much longer than in the compressive case a temperature criterion could not be used. Instead, the curves for a range of RRCs have been shown. Behaviour correlates well with an RRC value of 10% initially, suggesting that the laminate does not lose much strength until most of the resin has depleted. However, it appears that in cases where the tensile stress is below about 20% of the room temperature failure value, the structure can maintain load for quite a long time.

Model Predictions for the Fire Integrity of 'Generic' Composites

Measurements carried out on a range of different composite systems suggest that the differences in overall behaviour between different types of composite (even including phenolic) are not very large. The usual design requirement is to know the approximate time in a particular type of fire before collapse occurs. As an illustrative example therefore, the fire model has been used to generate predictions for the response of a 'typical' composite structure to a given fire threat. In these predictions it has been assumed that the failure mode is local compressive collapse, because this is the most probable mode of failure in any structure that is fully engulfed in fire. There will be some circumstances where these predictions are conservative, for instance when the loading is primarily tensile (as in the case of a pressurised pipe), or in a panel under flexure, with only the tensile face exposed. In defining the fire threat, we consider four broadly representative cases:

1. constant heat flux of 50 kWm^{-2}
2. constant heat flux of 75 kWm^{-2}
3. the cellulosic fire curve
4. the hydrocarbon fire curve.

The two constant heat flux conditions correspond respectively to a fully developed fire of moderate intensity and a rather hotter fire, such as a hydrocarbon pool fire. The standard fire curves are used in a range of tests where the temperature is increased in a prescribed way to imitate, albeit very approximately, a real fire scenario. The cellulosic curve represents a building fire and the hydrocarbon curve a hotter fire of the type that might be found in the petroleum industry. Figures 19–22 show the predictions of the model for all four fire scenarios, for collapse time under load (using the 170°C criterion) and for residual property retention after fire ($\text{RRC} = 80\%$). In each case, the integrity time has been shown vs. laminate thickness for 50 and 25% of residual integrity. The 25% value is of particular interest because, assuming a design factor of 4, this would correspond to collapse under the working load of the structure.

Figure 19 shows integrity under load for the two constant heat flux conditions. Interestingly, the relatively small difference between the curves for 50 and 75 kWm^{-2} underlines the non-linear effect of increasing heat flux, mentioned previously. Figure 20 shows the equivalent times corresponding to the two standard fire curves. The kinks in the curves are due to the 'start-up' and levelling off phases of the two standard curves. Once again, given the considerable difference in severity between the standard curves, there is surprisingly little difference between the integrity times. It is interesting to note that, for moderate laminate thicknesses, the 50 kWm^{-2} constant heat flux condition appears to be more severe than the hydrocarbon curve, due presumably to the effect of the start-up period.

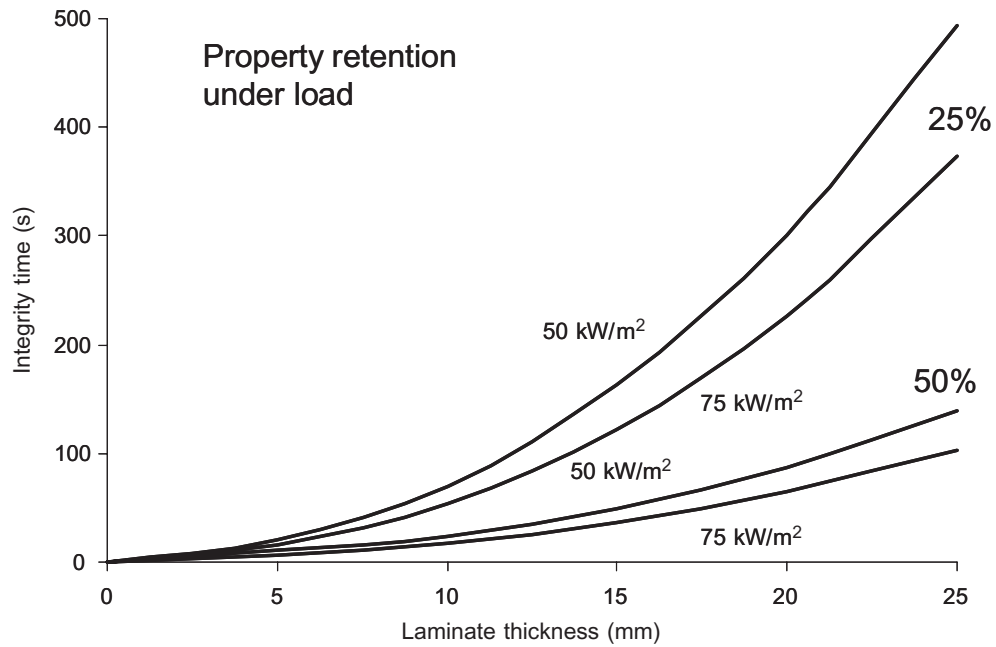


Figure 19. Predicted times for 50 and 25% retention of integrity under load for generic composite laminates. Type of fire exposure: 75 and 50 kW/m² constant heat flux. Model assumes that failure mode is buckling and that property loss occurs when laminate reaches 170°C.

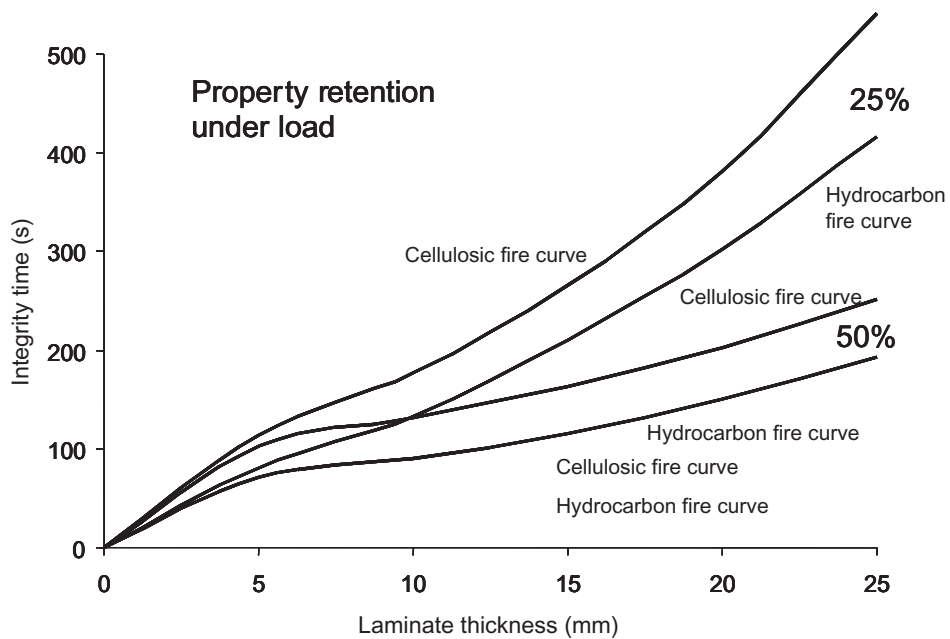


Figure 20. Predicted times for 50 and 25% retention of integrity under load for generic composite laminates. Type of fire exposure: 'cellulosic' and 'hydrocarbon' fire curves. Model assumes that failure mode is buckling and that property loss occurs when laminate reaches 170°C.

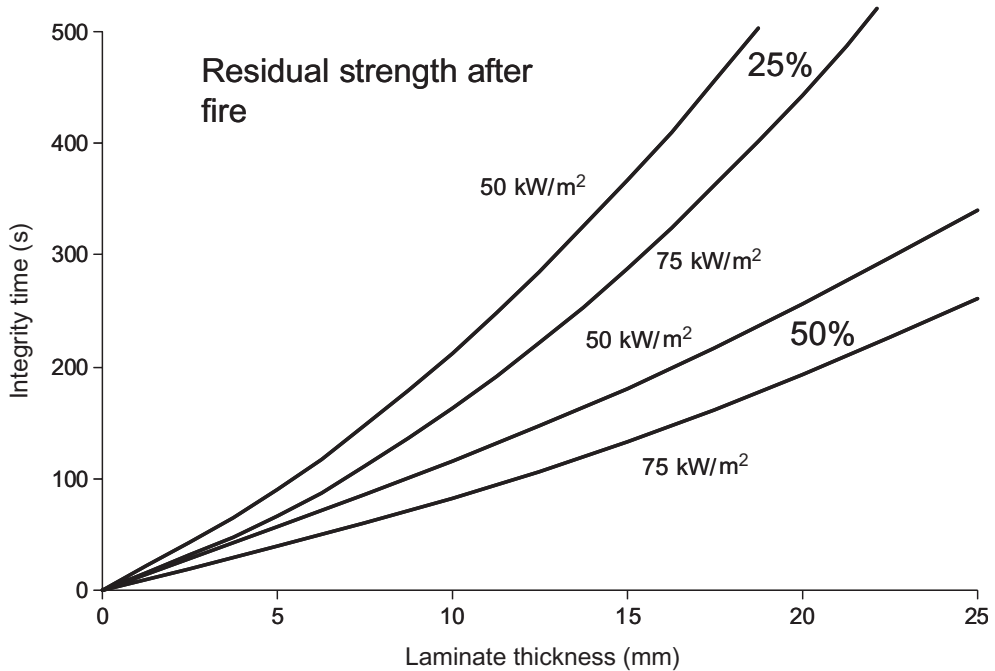


Figure 21. Predicted times for 50 and 25% retention of post-fire residual integrity for generic composite laminates. Type of fire exposure: 75 and 50 kW/m² constant heat flux. Model assumes that failure mode is buckling and that property loss occurs when laminate RRC reaches 80%.

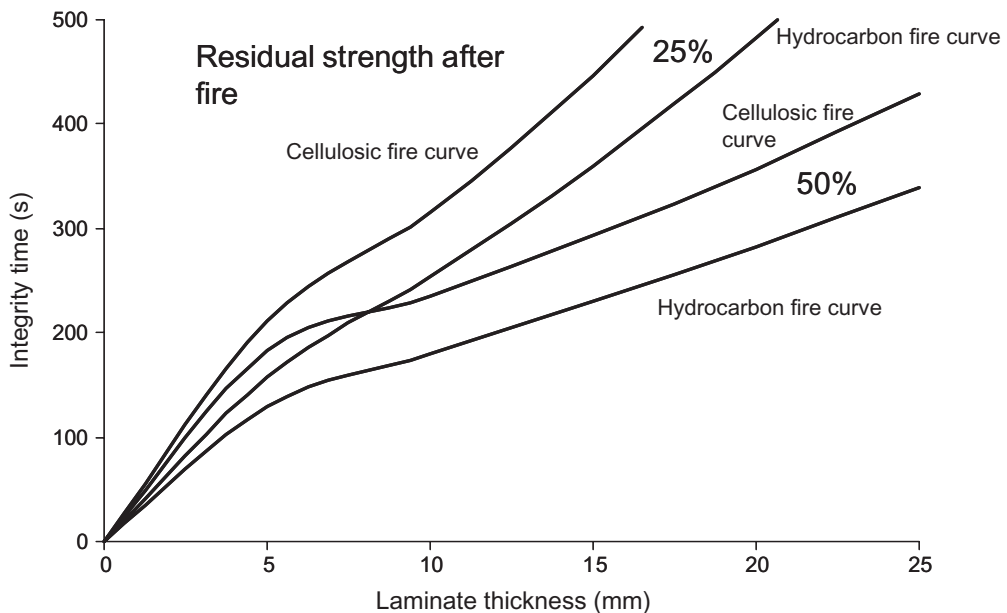


Figure 22. Predicted times for 50 and 25% retention of post-fire residual integrity for generic composite laminates. Type of fire exposure: 'cellulosic' and 'hydrocarbon' fire curves. Model assumes that failure mode is buckling and that property loss occurs when laminate RRC reaches 80%.

Finally, Figures 21 and 22 show the equivalent predictions for the case of residual integrity after fire. The curves in both cases are rather similar in shape to the curves for behaviour under load, except that the integrity times are generally 2–3 times as long.

DISCUSSION AND CONCLUSIONS

We acknowledge that the ‘two-layer’ model is an approximation because it ignores the finite thickness of the decomposition region, and the variation in mechanical properties through the unburnt portion of material. Nevertheless this approach has been shown to be useful in characterising both behaviour under load and residual properties after fire. It also has the advantage of providing structural information in a form that is readily usable by designers.

The present results support the use of this approach, and the thermal model for the decomposition response provides an additional insight into the degradation processes that take place through the thickness of the laminate.

The key conclusion of this work is that integrity times in fire are short and that composite structures are especially prone to local compressive failure. This underlines the need for appropriate protection, a solution that is also widely employed in the case of steel and aluminium structures.

We are working to extend the present investigation to take more accurate account of the full progressive change in properties through the thickness of laminates in fire.

ACKNOWLEDGEMENTS

The Newcastle University authors would like to acknowledge EPSRC funding (along with VT (UK) Ltd and Fiberline Composites) for the research programme on *Fire resistance of loaded composite structures* as well as the support of the EU *COMPOSIT* network. We also wish to thank Mr C. Townsend (DSTO) for assistance with specimen fabrication and cone calorimetry.

REFERENCES

1. Standard for Qualifying Marine Materials for High Speed Craft as Fire-restricting Materials, *Resolution MSC.40(64)*, International Marine Organisation, London, 1994.
2. ISO 9705, *Fire Tests – Full Scale Room Test for Surface Products*, 1991.
3. BS 6853, *Fire Precautions in the Design and Construction of Railway Passenger Rolling Stock*, 1987.
4. Epiradiateur and NFF-16-101, *French Surface Spread of Flame and Smoke Standard*.
5. BS 476, *Fire Tests on Building Materials and Structures*.
6. International Convention for the Safety of Life at Sea (SOLAS) 1974, Consolidated Edition 1992, IMO London (1992).
7. *Proceedings of Composites in Fire-3*, Sept. 9–10 2003, University of Newcastle upon Tyne, Publisher: Composite Link, UK. (CompositeLink@btconnect.com).
8. Pering, G.A., Farrell, P.V. and Springer, G.S. (1981). Degradation of Tensile and Shear Properties of Composites Exposed to Fire or High Temperature, In: Springer, G.S. (ed.), *Environmental Effects on Composite Materials*, pp. 145–159, Technomic Publishing Company Inc.

9. Griffiths, C.A., Nemes, J.A., Stonesifer, F.R. and Chang, C.I. (1986). Degradation in Strength of Laminated Composites Subjected to Intense Heating and Mechanical Loading, *Journal of Composite Materials*, **20**: 216–235.
10. Sorathia, U., Beck, C. and Dapp, T. (1993). Residual Strength of Composites During and After Fire Exposure, *Journal of Fire Science*, **11**: 255–270.
11. Sorathia, U., Lyon, R., Gann, R. and Gritz, L. (May/June 1996). Materials and Fire Threat, *SAMPE Journal*, **32**: 8–15.
12. Dao, M. and Asaro, R.J. (1999). A Study on Failure Prediction and Design Criteria for Fiber Composites under Fire Degradation, *Composites*, **30A**: 123–131.
13. Mouritz, A.P. and Mathys, Z. (2000). Mechanical Properties of Fire-damaged Glass-reinforced Phenolic Composites, *Fire and Materials*, **34**: 67–75.
14. Mouritz, A.P. and Mathys, Z. (1999). Post-fire Mechanical Properties of Marine Polymer Composites, *Composite Structures*, **47**: 643–653.
15. Mouritz, A.P. and Mathys, Z. (2001). Post-fire Mechanical Properties of Glass-reinforced Polyester Composites, *Composites Science and Technology*, **61**: 475–490.
16. Gardiner, C.P., Mouritz, A.P., Mathys, Z. and Towsend, C.R. (Nov 2002). Tensile and Compressive Properties of GRP Composites with Local Heat Damage, *Applied Composite Materials*, **9**(6): 353–367.
17. Gibson, A.G., Wu, Y.S., Chandler, H.W., Wilcox, J.A.D. and Bettess, P. (Jan–Feb 1995). A Model for the Thermal Performance of Thick Composite Laminates in Hydrocarbon Fires, *Composite Materials in the Petroleum Industry*, Revue de l'Institut Français du Pétrole (Special Issue), **50**(1): 69–74.
18. Dodds, N., Gibson, A.G., Dewhurst, D. and Davies, J.M. (2000). Fire Behaviour of Composite Laminates, *Composites, Part A*, **31**: 689–702.
19. Looyeh, M.R.E., Bettess, P. and Gibson, A.G. (1997). A One-dimensional Finite Element Simulation for the Fire Performance of GRP Panels for Offshore Structures, *Int. J. of Numerical Methods for Heat and Fluid Flow*, **7**(6): 609–625.
20. Gibson, A.G., Wright, P.N.H., Wu, Y-S., Mouritz, A.P., Mathys, Z. and Gardiner, C.P. (2003). Modelling the Residual Properties of Polymer Composites after Fire, *Plastics, Rubber and Composites*, **32**(2): 81–90.
21. ASTM D3039M-95A. *Annual Book of ASTM Standards*, Vol. 15.03; 1996 PA, American Society for Testing and Materials.
22. ASTM D970. *Annual Book of ASTM Standards*, Vol. 18.01; 1996 PA, American Society for Testing and Materials.
23. ASTM E457-96 (1996). Standard Test Method for Measuring Heat Transfer Rate Using a Thermal Capacitance (Slug) Calorimeter. *American Society for Testing and Materials*, PA.
24. *Advanced Composite Compression Tests*, Boeing Specification Support Standard, BSS 7260, 1986.
25. Bamford, C.H., Crank, J. and Malan, D.H. (1946). The Combustion of Wood, Part 1, *Cambridge Phil. Soc. Proc.*, **42**: 166.
26. Henderson, J.B., Weibelt, J.A. and Tant, M.R. (1985). A Model for the Thermal Response of Polymer Composite Materials with Experimental Verification, *Journal of Composite Materials*, **19**: 579–595.
27. Henderson, J.B. and Wiecek, T.E. (1985). A Mathematical Model to Predict the Thermal Response of Decomposing, Expanding Polymer Composites, *Journal of Composite Materials*, **21**: 373–393.
28. Milke, J.A. and Vizzini, A.J. (1991). Thermal Response of Fire Exposed Composites, *Journal of Composites Technology and Research*, **13**: 145–151.
29. Kansa, E.J., Perlee, H.E. and Chaiken, R.F. (1977). Mathematical Model of Wood Pyrolysis Including Forced Convection, *Combustion and Flame*, **29**: 311–324.
30. Adams, M.C. (1959). Recent Advances in Ablation, *American Rocket Society*, **29**: 9.
31. Anilturk, D. and Chan, W.S. (2003). Structural Stability of Composite Laminated Column Exposed to High Temperature of Fire, *Journal of Composite Materials*, **37**(8): 687–700.

32. Bausano, J., Boyd, S., Lesko, J. and Case, S. (2003). Composite Life Under Sustained Compression and One Sided Simulated Fire Exposure: Characterisation and Prediction, *Composites in Fire-3*. Reference 7 above.
33. Lua, J. and O'Brien, J. (2003). Fire Simulation for Woven Fabric Composites with Temperature and Mass-Dependant Thermal Mechanical Properties, *Composites in Fire-3*. Reference 7 above.
34. *Roark's Formulas for Stress and Strain*, 6th edn., (1989). In: Young, W.C. (ed.), McGraw-Hill, New York.
35. Eckold, G. (1994). *Design and Manufacture of Composite Structures*, Woodhead Publishing Ltd, Cambridge.
36. Stausky, Y. and Hoff, N.J. (1969). Mechanics of Composite Structures. In: Dietz, A.G.H. (ed.), *Composite Engineering Laminates*, pp. 5–59, MIT Press, Cambridge Mass.

